SUBJECT: **SPIRE Photometer Point Source Mode Status (ICC Review)**

PREPARED BY: Chris Pearson

Andreas Papageorgiou, Bruce Sibthorpe, Ivan Valtchanov

On behalf of the Jiggle Validation Group

DOCUMENT No: SPIRE-RAL-DOC-003244

ISSUE: 1.0 Date: 29th January 2010

APPROVED BY: Date:

Distribution

SPIRE ICC	

Change Record

ISSUE	DATE	Changes
Draft 1.0	25 January 2010	

1 INTRODUCTION

1.1 Structure of this Document

This document contains a summary of the status of the SPIRE Photometer Point Source mode. Currently this mode is not released, and the observations necessary to optimise the mode are continuing. This document gives a brief summary of the operation of the mode, including the definition of the uplink parameters, calibration, pipeline and preliminary data.

1.2 Documents

1.2.1 Applicable Documents

1.2.2 Reference Documents

RD1	SPIRE Pipeline Description Document SPIRE-RAL-DOC-002437
RD2	The SPIRE Analogue Signal Chain and Photometer Detector Data Processing Pipeline SPIRE-UCF-DOC-002890

2 PHOTOMETER POINT SOURCE MODE

The photometer point source mode (also referred to as the **7-pt Jiggle** mode or **POF2** mode) is the SPIRE observation mode optimized for the observation of point sources. The mode involves movement on and off the source so therefore this mode is ideally suited to sources with well known positions and relatively bright expected fluxes.

2.1 Chopping, Nodding & Jiggling

The observation requires both chopping and Nodding as shown below schematically in Figure 1;

- **Chopping:** Chopping is made on and off source with the Beam Steering Mirror to modulate the signal to obtain a difference signal (background + source in one, just background in the other).
- **Nodding:** The telescope is physically nodded to remove asymmetries in optics and in background thermal radiation field (the telescope).
- **Jiggling:** The ensure correct sampling of the source a 7-point Jiggle pattern is carried out at each chop position using the BSM (See Figure 2)

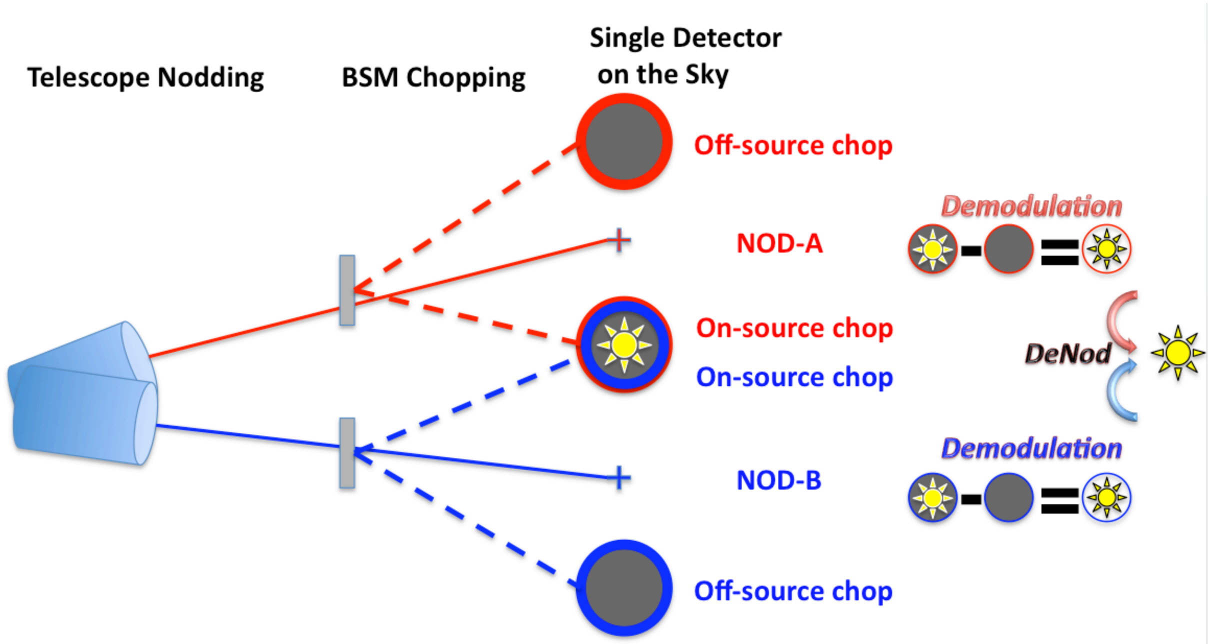

Figure 1: *Schematic overview of the Point Source Mode showing the different steps of chopping and nodding in this observation mode*

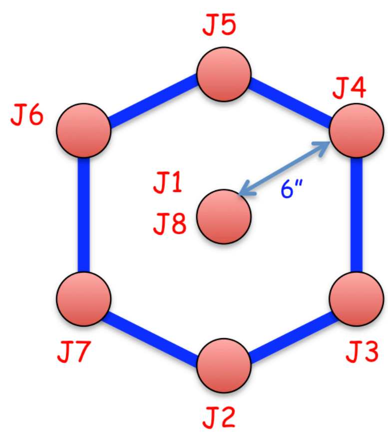

Figure 2: *The pattern traversed by a detector around the 7-point Jiggle Pattern. Note the first and the final positions are identical.*

During a single observation 3 co-aligned detectors (i.e. co-aligned detectors for all PSW, PMW, PLW arrays) see the source, with the central co-aligned detector seeing the source on BOTH Nod cycles (See Figure 3). The adopted parameters are described in Table 1.

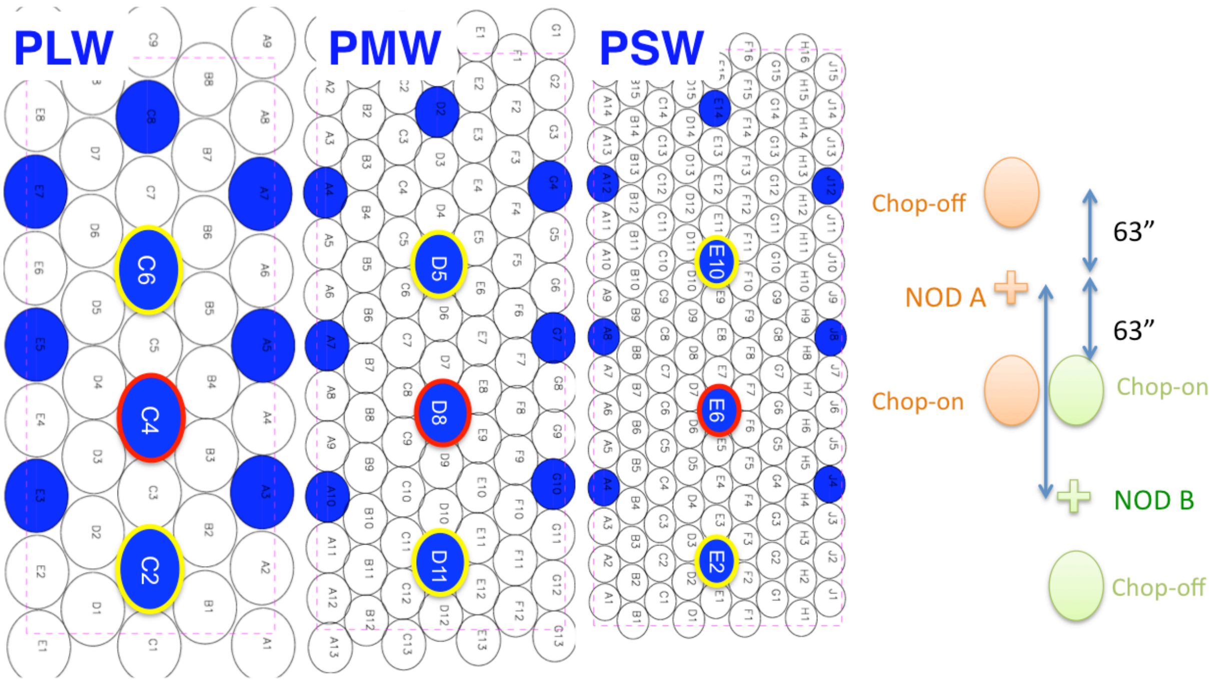

Figure 3: The photometer detector arrays showing all co-aligned detectors (blue).*The detectors on the 3 photometer arrays that are used during the Point Source Observation Mode shown as red and yellow. The central prime detector (red, PSWE6, PMWD8, PLWC4) sees the source on both Nod cycles while each of the secondary detectors (yellow) see the source on a single Nod Cycle. During an observation some detectors (denoted by those outside the pink dotted box in the figure are chopped off the sky and see the inside of the instrument.)*

Table 1: *Adopted parameters for Point Source observation mode*

Parameter	Value
Chop throw	126 arcsec
Nod Distance	126 arcsec
Chopping frequency	1Hz *
Jiggle pattern separation	6 arcsec
Prime detectors	PSWE6, PMWD8, PLWC4
Secondary (upper) detectors	PSWE10, PMWD5, PLWC6
Secondary (lower) detectors	PSWE2, PMWD11, PLWC26

* Changed from pre-launch value of 0.5Hz for better chop stability.

2.2 Operation and Uplink

One repetition of the Point Source mode 7-point Jiggle AOR is defined a one set of ABBA Nod cycles (i.e. Nod to position A, Nod to position B, stay at position B, Nod back to position A). The mode then carries out a set of 8 on-source/off-sourcechop cycles as it moves around the 8 positions Jiggle Pattern (jiggle positions 1 – 7 then back to position 1 as in Figure 2). The operation is described in detail below;

1. First nod position (**Nod A**)
   - At 1/8 jiggle position - Chop on/off source (8 chop cycles at 1 Hz)
   - At 2/8 jiggle position - Chop on/off source (8 chop cycles at 1 Hz)
   - ………………..
   - At 8/8 jiggle position - Chop on/off source (8 chop cycles at 1 Hz)
2. Nod to second position (**Nod B**) and repeat
   - At 1/8 jiggle position - Chop on/off source (8 chop cycles at 1 Hz)
   - At 2/8 jiggle position - Chop on/off source (8 chop cycles at 1 Hz)
   - ………………..
   - At 8/8 jiggle position - Chop on/off source (8 chop cycles at 1 Hz)
3. Stay in **Nod B** and repeat
   - ………………..
4. Nod to **Nod A** and repeat
   - ……………

These commands is carried out as a set of observational building blocks. A building block is the fundamental element of any SPIRE observation. For the point source mode the building blocks are either a command to Nod or a command to carry out a number of chop cycles at one given Jiggle Position. The building block structure for a single ABBA Nod cycle of the point source mode is shown in with the typical timings associated with a given building block.

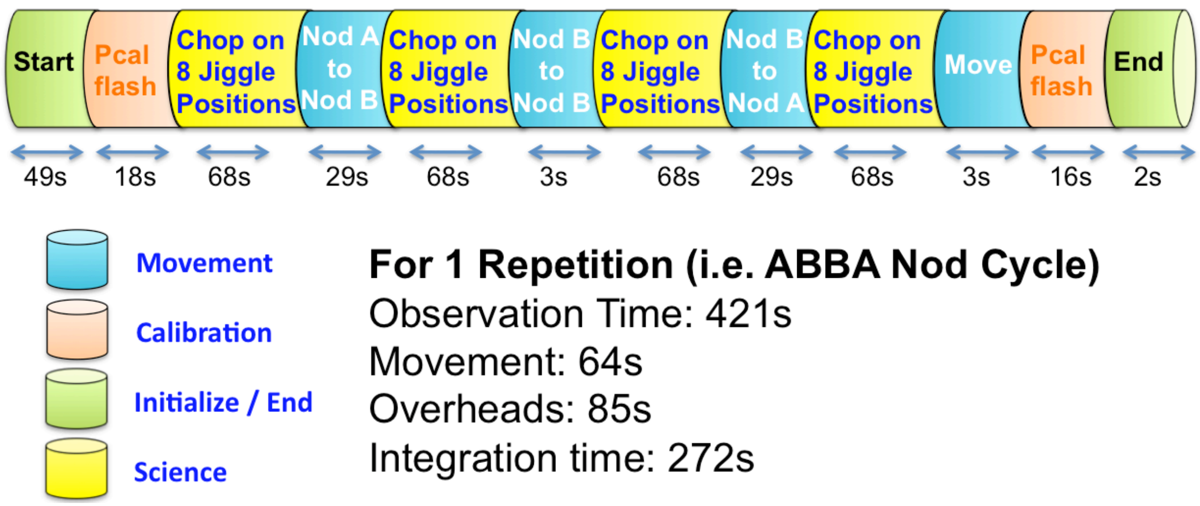

Figure 4: *Building Block commands defining a single ABBA repetition of the Point Source observation mode with associated timings.*

3 BSM COMMANDED POSITIONS AND BEHAVIOUR

3.1 BSM Operations Calibration File

The 7- point Jiggle Pattern is described by the *BSM Operations* Calibration File, which defines;

- Chop Throw (set at ±63 arcsec)
- Jiggle positions and ordering
- Jiggle spacing (set at 6 arcsec)

The BSM Operations file holds these values in the form of BSM Chop and Jiggle sensor values (0 - 65536) where the “chop” axes is aligned with the Y-axis in the focal plane and the “jiggle” axis is aligned with the Z-axis of the focal plane. Both the chop-throw and the individual jiggle positions are original defined in terms of –Y –Z plane angles in arcsecs and these values have to be converted into the corresponding Chop and Jiggle BSM sensor values. This conversion is carried out by the *BSM Positions* Calibration file that holds a look up table containing the corresponding sensor value for a given angle in the focal plane. In Figure 5 the uplink for the 7 point jiggle pattern derived from flight data is shown in both angle and BSM sensor units. A very small shift is seen for the updated calibration compared with the pre-flight values. The calibration of the BSM (sensor value to angle conversion) is made by slowly scanning the BSM across the array over a bright source and noting the BSM sensor value when the source is detected on a given detector (whose angular position in the focal plane is known).

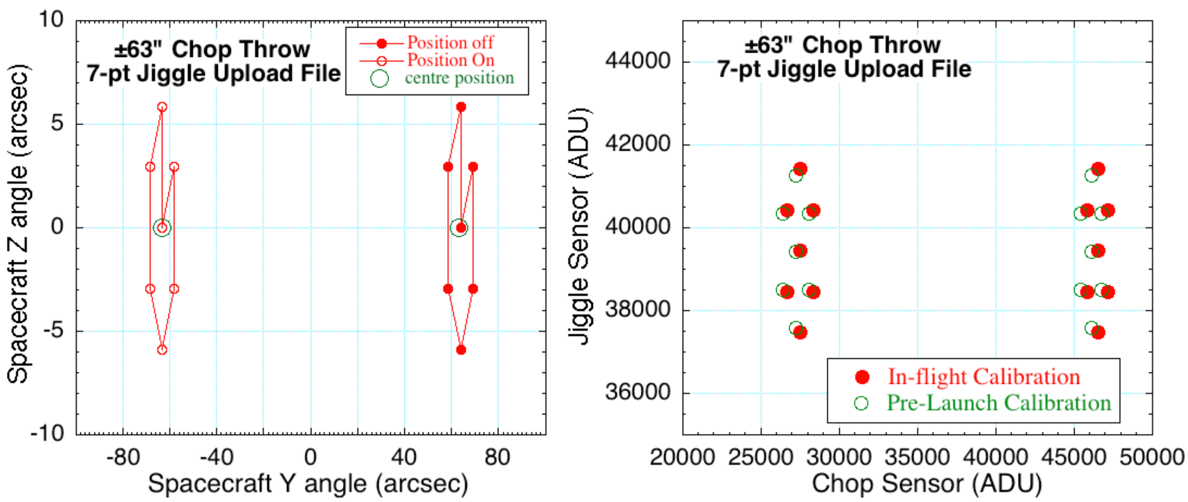

Figure 5: *The template for the 7-point Jiggle pattern (with a chop throw of 126 arcsec) in the original angle pattern (left) and the calibrated BSM sensor pattern (right). Note that there is a slight shift in the pattern compared to what was measured on the ground.*

3.2 The in-flight stability of the BSM

The fundamental accuracy of the 7-point Jiggle Point Source Mode critically depends upon the stability of the BSM since both the movement between chop-cycles and movement around the 7-point Jiggle pattern are implemented by the motion of the BSM. After launch the BSM was found to be not optimally tuned and that in many cases, although the BSM was sent to the correct position. It did not quite reach it. To try and improve the BSM performance, tuning observations were carried out (adjusting the amount of overshoot, dampening etc). The results are shown in Figure 6. It can be seen that although the BSM performance is significantly improved, the first half of the BSM motion during any given chop cycle is still not stable and that moreover, it is very difficult to tune both chop beams simultaneously.

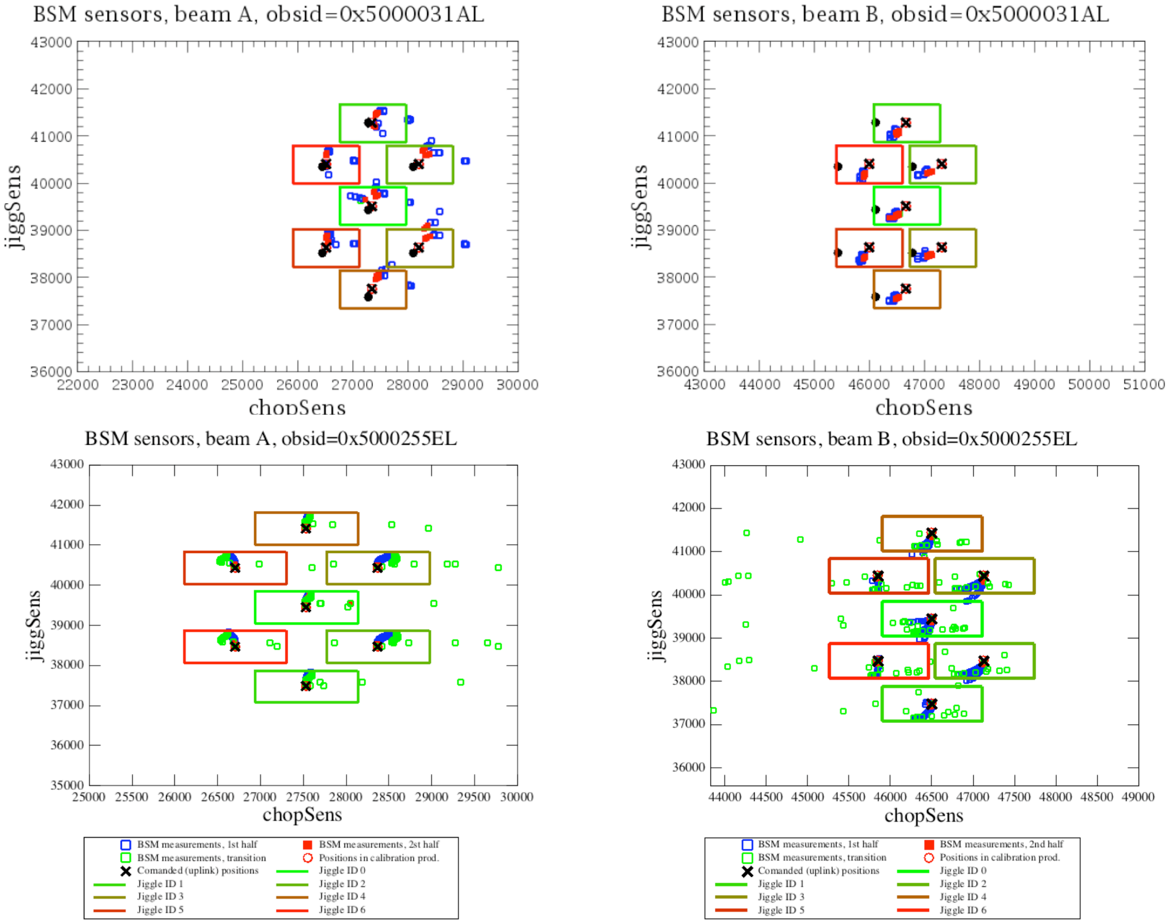

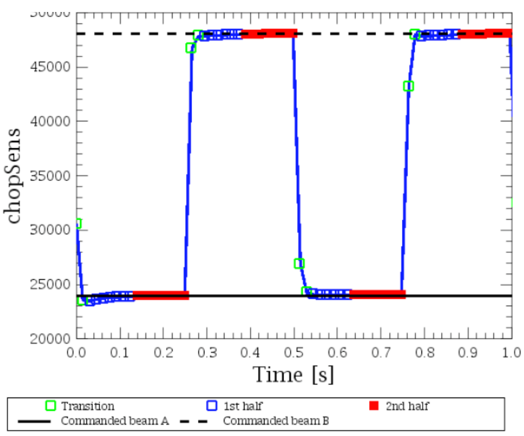

Figure 6: *Tuning of the BSM for the 7-point Jiggle pattern for the 2 chop beams (referred to as A & B although it should be noted in this case we are referring to chop-beams rather than Nodding, i.e. all motion is due to the BSM). Upper panels show the performance of the BSM after launch and the middle panels the performance of the BSM after tuning. The black crosses and red circles represent the commanded uplink and on board calibration positions respectively. The squares show the motion of the BSM (ignoring the green squares which are while the BSM is in transition and not shown on the upper panels) on the first half of a chop cycle and the second half of the chop cycle (shown in the left panel as the chop-sensor timeline for ~2 chop cycles). Tolerance limits for pipeline processing are shown as rectangular boxes around each Jiggle position. In the upper panels the BSM never reaches the target position. The middle panels, after tuning show improved performance although the first half of the chop cycle is still unstable, especially for the beam B. The BSM is extremely difficult to tune simultaneously for both chop beams.*

4 DOWNLINK

A description of the Pipeline Processing and Calibration File updates

4.1 Pipeline

The data from the Point Source Observation mode is processed by the standard data processing pipeline within the HIPE environment. The pipeline has been validated that the algorithms are correct but changes have still been made after launch to attempt to deal with the in-flight data. The raw telemetry (Level 0 data) is processed through an engineering conversion to Level 0.5 where the data is in the form of voltage timeline data. Figure 8 shows the standard POF-2 pipeline for the point source mode (see AD1 for a detailed description of the processing steps and calibration files). Input is assumed to be the voltage calibrated Level 0.5 Photometer detector timeline products. Processing steps are shown in blue, Level 0.5, 1, 2 data products in yellow, intermediate data products in green and calibration files in orange. The processing steps are outlined below;

- Level 0.5 Product: Photometer Detector Timeline Products as Calibrated voltage timelines.
  - Remove electrical crosstalk - matrix function (electrical cross talk <0.1%)
  - First Level Deglitching - wavelet analysis
  - Flux conversion -described in RD2
  - Associate Sky Position – attached RA and Dec timelines
  - Demodulation – demodulate the on and off target chop positions to remove background (The demodulation module was upadated to cope with the BSM instability in Figure 6)
  - Second Level Deglitching and averaging – average the 8 chop cycles at each Jiggle position and perform outlier rejection
  - De-Nod: De-nod the ABBA Nod positins
  - Remove Optical Crosstalk - matrix function (negligable)
  - Average Nod Cycles – average the data from all sets of ABBA cycles
- Level 1 Product: Averaged Pointed Photometer Product as set of 7+1=8 Jiggle positions flux/position (see **Figure 7**)
  - Point Source Fit – Gaussian fit to flux and positions of individul Jiggle positions
  - Mapmaking – Sparse map of bolometers
- Level 2 Product: Jiggled Photometer Product as a single flux/position for each array (**Figure 7**)
- Level 2 Product: Photometer Map Product as a sparse map of bolometers (see **Figure 7**)

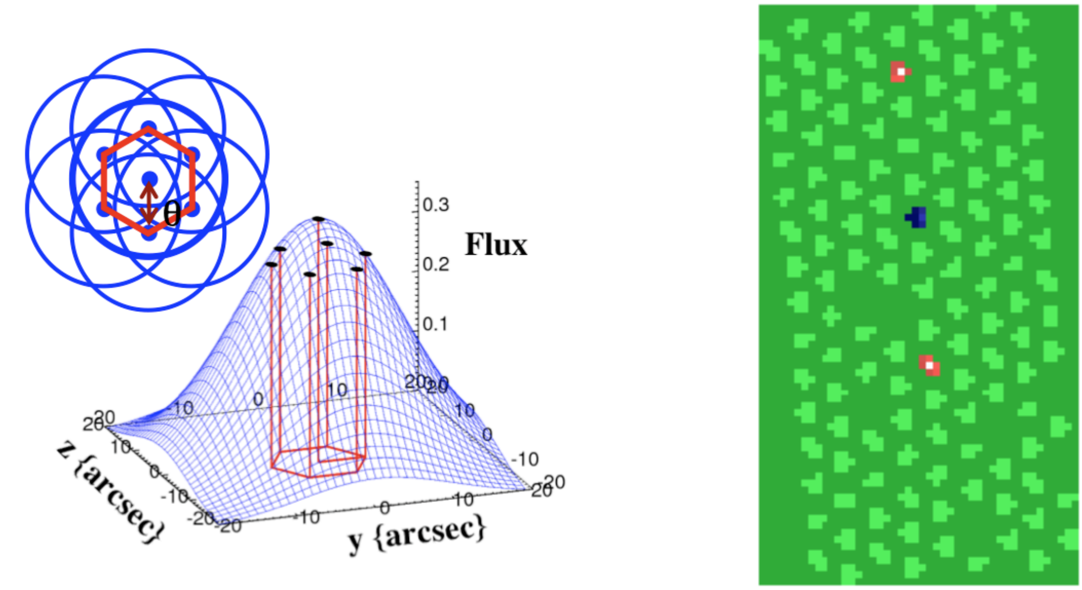

Figure 7: *Final Level 1 and Level 2 products. (*left*) the Level 2 Jiggled Photometer Product is a single flux/position calculated by fitting a Gaussian to the Level 1 Averaged Pointed Photometer Product which holds the flux and position calculated for each of the 8 Jiggle positions. (*right*) sparse map showing the PSW array with the on-target and 2 off target chop positions clearer visible.*

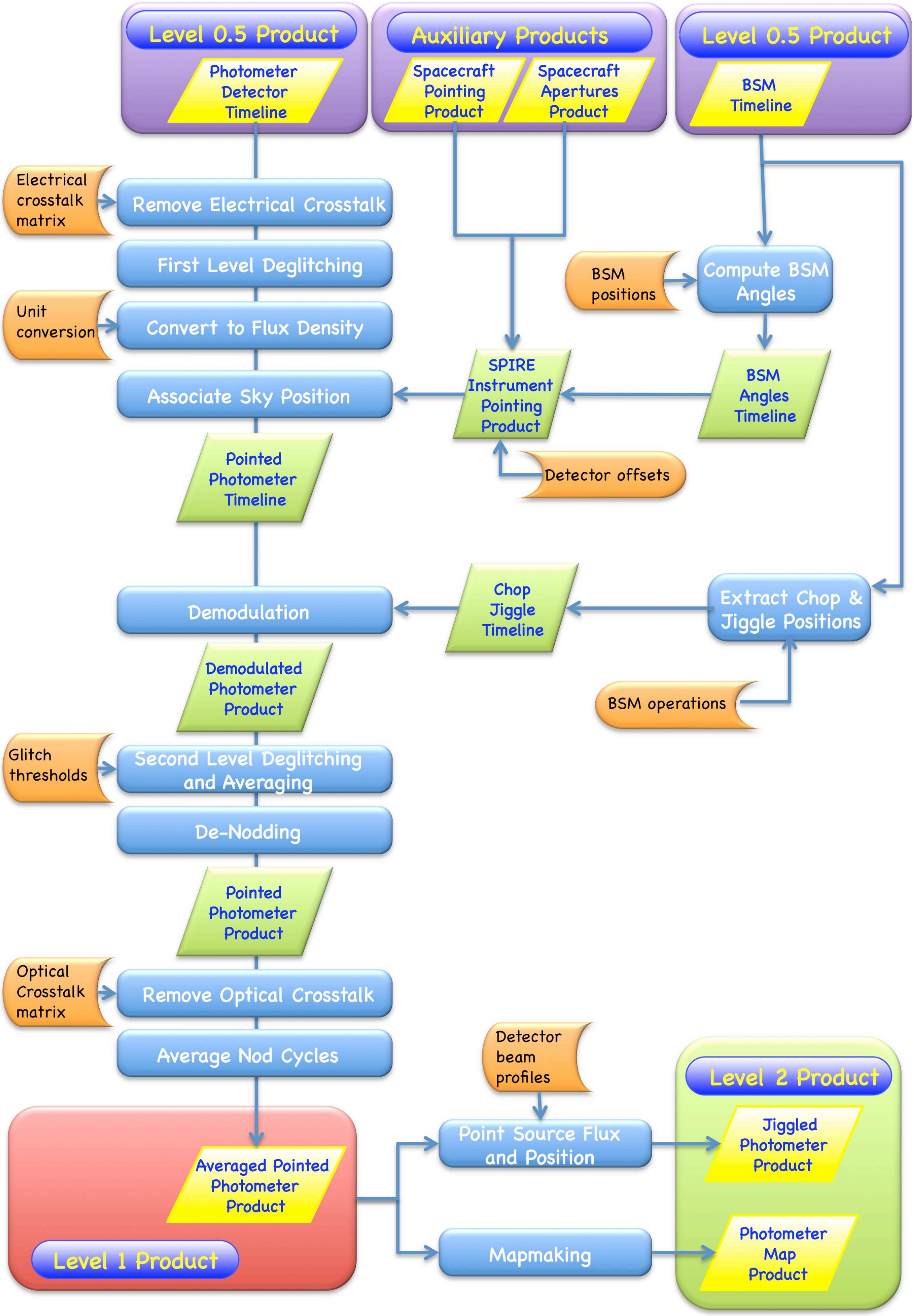

Figure 8: *Standard POF-2 pipeline for the point source mode. Input is assumed to be the voltage calibrated Level 0.5 products. Processing steps are shown in blue, Level 0.5, 1, 2 data products in yellow, intermediate data products in green and calibration files in orange.*

4.2 Calibration and Calibration Files

Updated calibration files derived from the analysis of flight data were provided during commissioning and PV phase:

- BSM Operations File & BSM Positions File:
  Updated Sept 09 with calibration on Alpha Ori
  Updated Nov 09 with calibration on Neptune

- Detector Angular Offsets Table (angular positions of detectors in focal plane in arcsec):
  Updated Aug 09 with an inversion of Y,Z angles after comparison with flight data
  Updated Sept09 with values from fine scan observations of 3C273

- Flux Calibration:
  Updated Sept 09 after early observations of Ceres
  Updated Nov 09 after observations of Neptune

5 PERFORMANCE

5.1 Point Source Mode Observations

Many nominal observations were made during PV phase on point sources ranging in flux from 160Jy to 0.2Jy including observations to verify the flux calibration. The performance of the mode is discussed below in Section **Error! Reference source not found.**.

In addition observations were made to investigate the optimization of the mode including;

- Nodding in the opposite direction (to place the target source on a different set of bolometers)
- Changing the separation of the Jiggle position (Testing separations of 5, 6, 7, 8, 9 arcsec)
- Changing the number of cycles around the Jiggle pattern for a given Nod to test the stability of the background emission of the system.

  In all cases, no significant advantage was found over the nominal operation of the Point Source Mode.

5.2 Flux Accuracy and Positional Performance

A straight-forward check of the performance of the point source mode can be made by directly comparing the measured flux from the POF-2 Level 2 product (the point source fit to all 8 Jiggle positions) with observations made by the Scan Map mode of the same target and/or predictions from pre-flight modelling. In Figure 9 the POF-2 pipeline flux general reproduces the flux values observed in other modes or models, with the level of agreement varying between 5-20%.

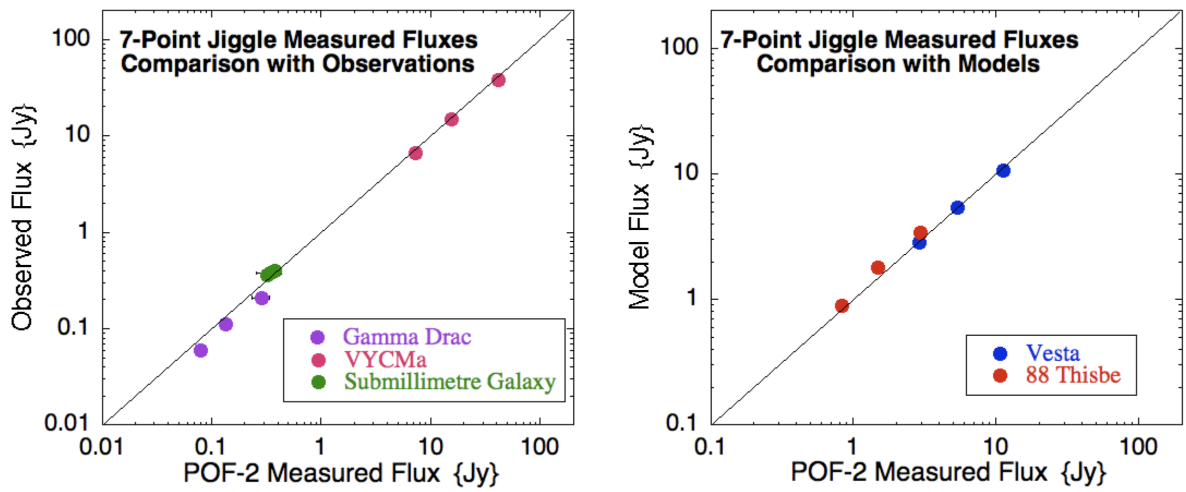

Figure 9: *A comparison of the flux measured in Point Source Mode with fluxes for the same targets (left) measured by observation (e.g. Scan-Map Mode) or (right) compared to model predictions. Note that Neptune was also observed and the flux agreed with observations and model predictions but some bolometers were saturated therefore the points are not shown.*

Positional accuracy can be checked by comparing the measured angular separation from the fitted positions from the POF-2 Level 2 product with the original uploaded commanded positions. In general it is found that the final Positional accuracy of the fitted source can vary from 1 ~ 5 arcsec, with the majority of sources having an accuracy of ~2 arcsec.

5.3 Stability and Repeatability

An analysis of the errors in the pipeline and the stability of the measured flux as a function of the number of Nod Cycles (i.e. effectively the integration time) has shown that there still exists an inherent instability in the observation mode and that the errors are still not well understood. In Figure 10 the Level 1 product estimated flux and the associated uncertainty for a given Jiggle position, as a function of increasing number of Nod Cycles (ie, integration time) is shown for Alpha Ori (~5Jy source). For an ideal system, the average flux is expected to be constant as a function of increasing Nod Cycles while the error is expected to decrease as a function of the reciprocal of the square root of the number of Nod Cycles eventually reaching a plateau. Although, in general the average flux is constant there are variations even at high numbers of Nod Cycles of >100mJy, moreover for the errors the "apparent" plateau reached faster in the case of Jiggle position 6, relative to Jiggle position 1 and the error at some Jiggle positions change in a strange manner (e.g. Jiggle Position pos 3 in Figure 10).

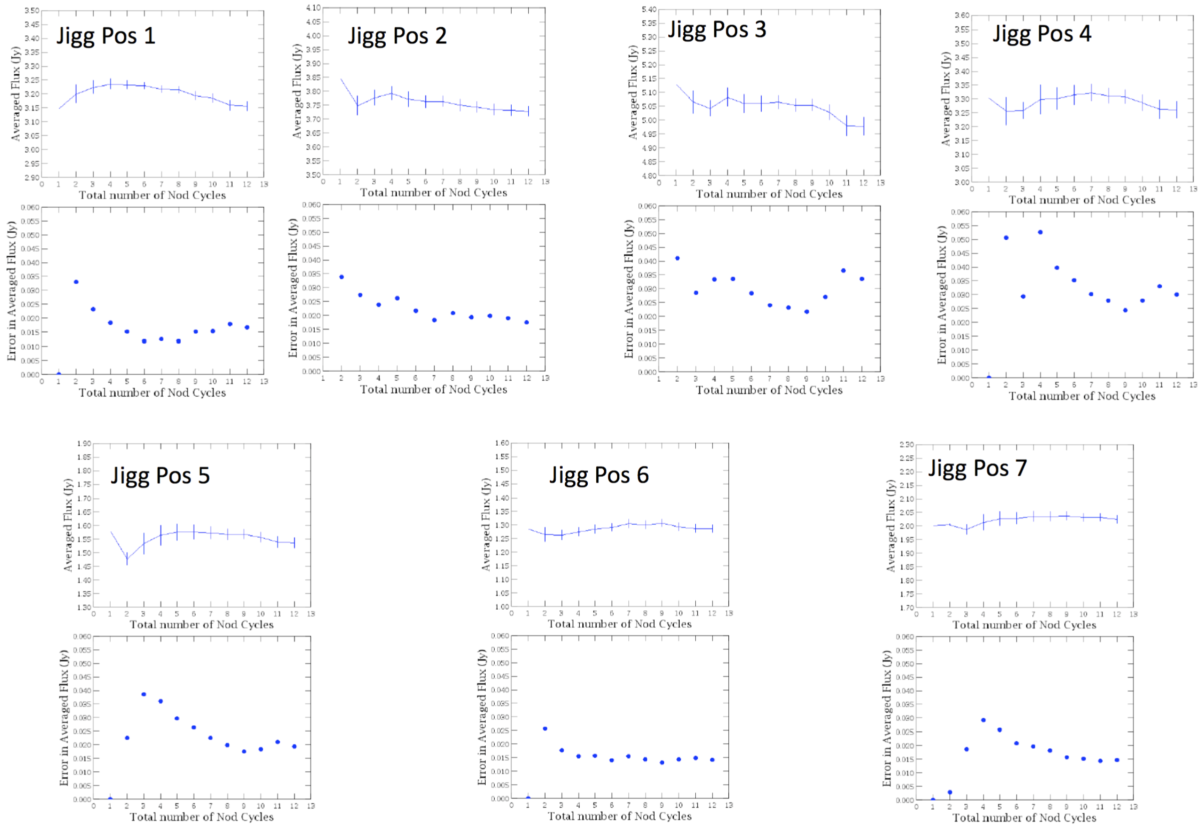

Figure 10: *Pipeline estimated flux (and associated uncertainty) for a given Jiggle position, as a function of increasing number of Nod Cycles (ie, integration time). Top panels: averaged flux against cumulative number of Nod Cycles. Bottom Panels: error on averaged flux against cumulative number of Nod Cycles.*

Note that Figure 10 is an integral plot and the instability in the system can be emphasized by looking at the measured signal on each individual Nod Cycle. This differential quantity is plotted in Figure 11 for the same target Alpha Ori. The instability in the signal for different Nod cycles is clear with dispersions of >100mJy in some cases and a seemingly downward trend at higher Nod cycles. Note also that the source is actually detected on Jiggle Position 3 rather than the central Jiggle position.
Figure 12 shows the Level 2 Product (Point Source Fit) for the Alpha Ori target. The left panel shows the positional offset in RA and Dec from the commanded position. The offsets are of the order of a few arcsecs, consistent with the pointing accuracy of the telescope. The right panel shows the final fitted flux as a function of Nod Cycle (individual values rather than cumulative values). A dispersion of up to 200mJy can be seen from nod cycle to nod cycle indicating an instability at some point in the system.
The RMS flux value for this observation are at the ~100mJy level

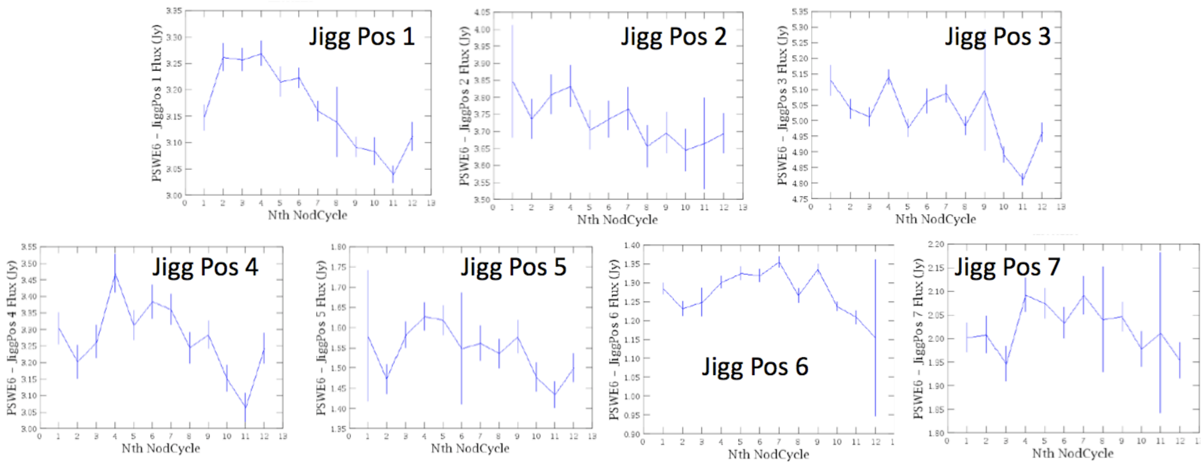

Figure 11: *The Level 1 Product flux measured on individual Nod Cycles at each Jiggle Position for a total of 12 Nod Cycles (Alpha Ori)*

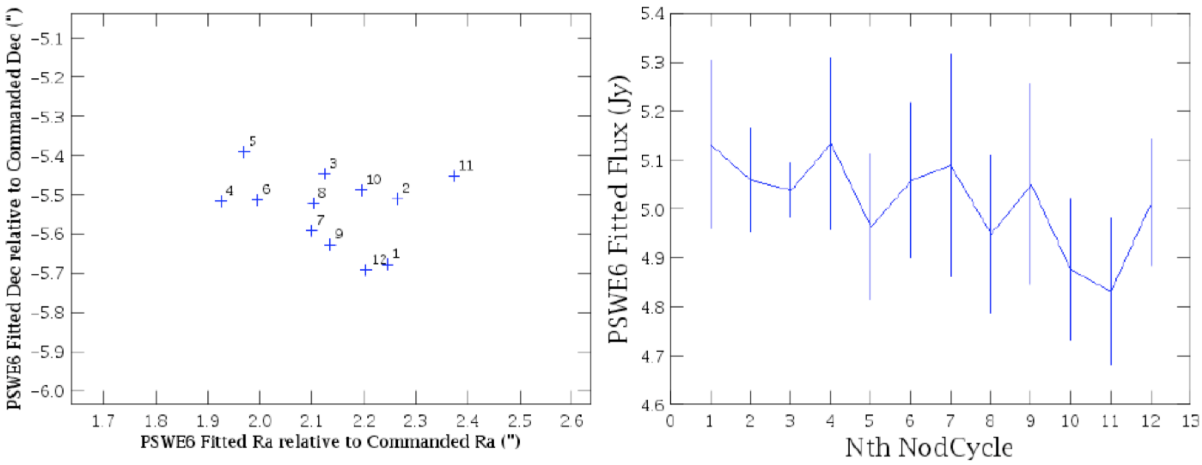

Figure 12: *The Level 2 Product (Point Source Fit) for the Alpha Ori target. The left panel shows the positional offset in RA and Dec from the commanded position. The right panel shows the final fitted flux as a function of Nod Cycle (individual values rather than cumulative values).*

6 Current Status of Point Source Mode

Currently, this mode will not be released until the uncertainties in the system have been identified and analysed.

6.1 Instabilities introduced by the BSM

Chopping and movement around Jiggle pattern depends on the tuning and stability of the BSM. It is already known that presently the BSM cannot be tuned optimally for both chop beams and that moreover the tuning required for each of the individual Jiggle positions is different. In Figure 13 the BSM chop sensor timeline is shown for a few of the Jiggle positions in the Level 0.5 data (i.e. before demodulation and De-Nodding). Ideally the modulated chop signal should be a square wave but instead an overshooting of the BSM is seen at both the on-source and the off-source positions is seen. Moreover the BSM never quite reaches a stable plateau on a given chop cycle. This instability in the BSM has a corresponding effect on the signal of the data as shown in Figure 14 which plots the the Level 0.5 data detector data. The signal on a given chop plateau varies significantly with peak to trough values on a single chop plateau reaching 100mJy.

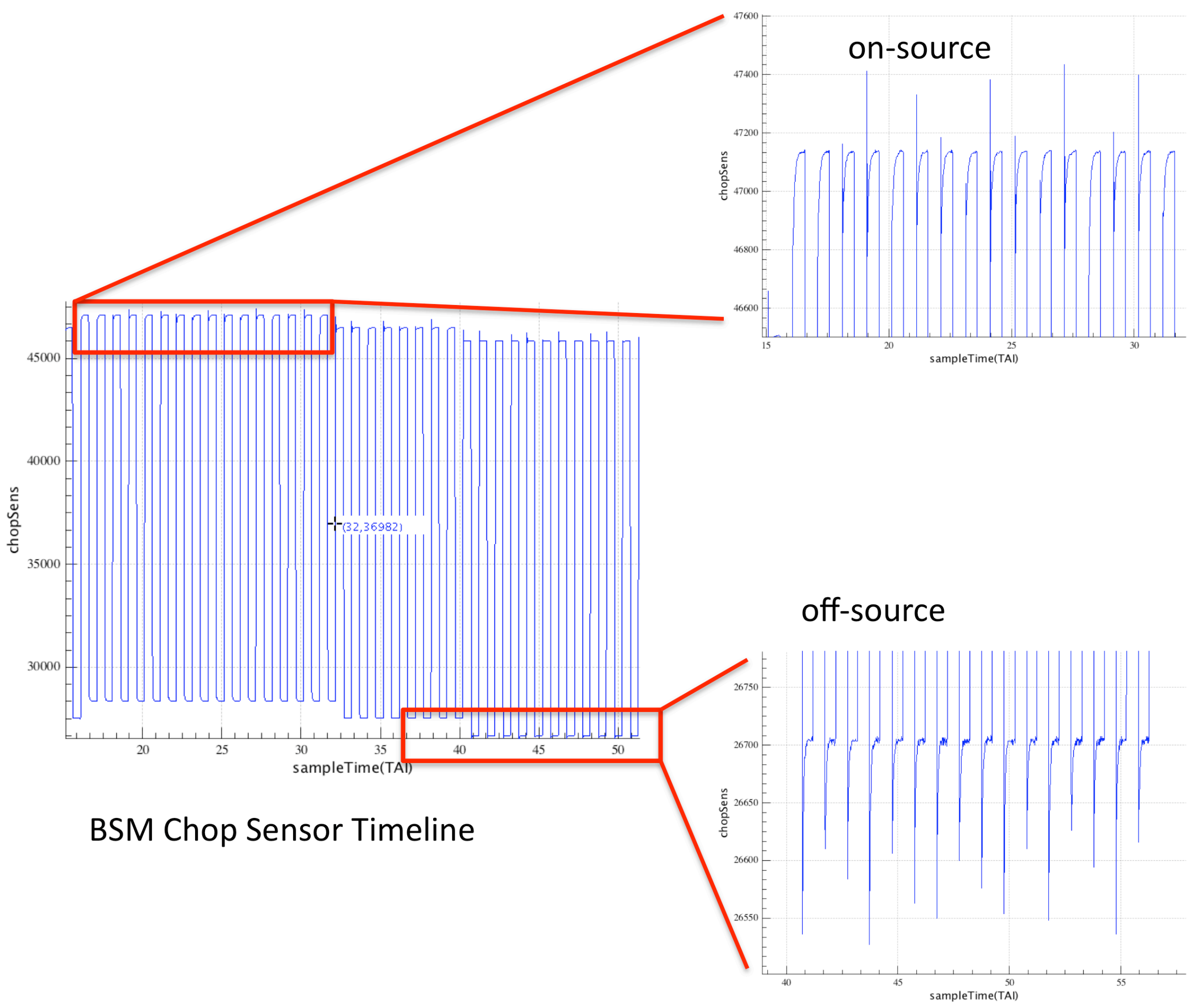

Figure 13: *The BSM Chop Sensor timeline showing that even chopping at 1Hz the BSM is still unstable and never truly settles. The on source and off source chop beams are shown enlarged.*

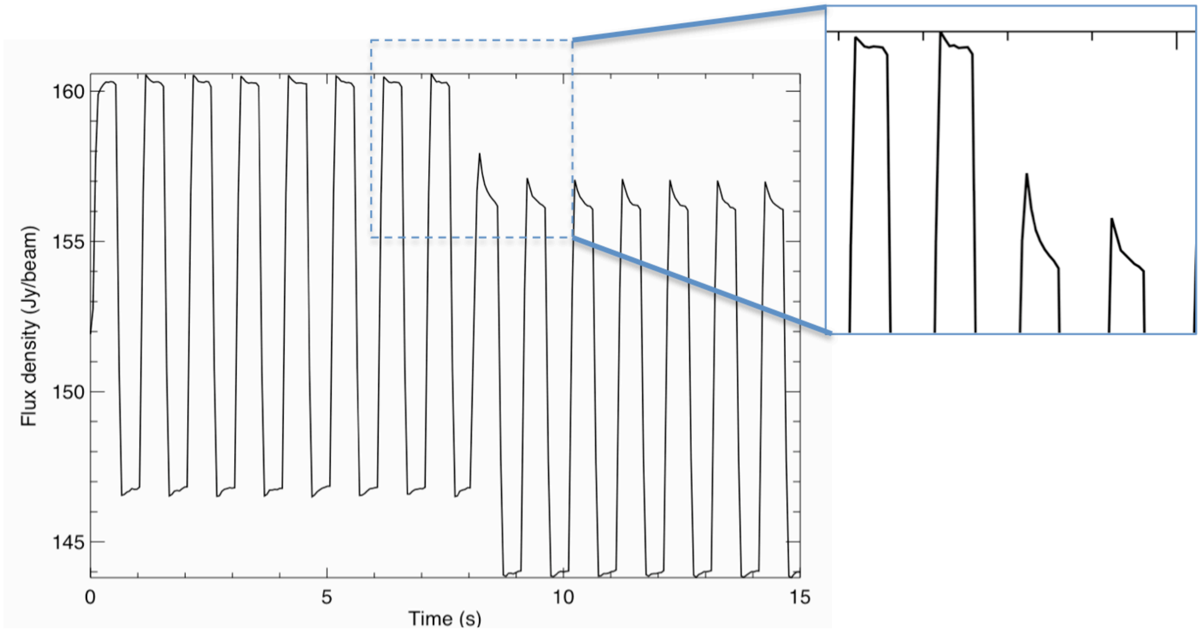

Figure 14: *The signal in the Level 0.5 modulated data showing the fluctuation caused by the motion of the BSM. In the enlarged image on the right a peak to trough difference of as much as 100mJy is apparent.*

The instability in the BSM for individual chop cycles imposes a fundamental limit on the errors and repeatability of this mode at present which blocks the release of this mode to the community.
A large scale test observation was carried out on the BSM in flight on Operational Day 196 (25th November 2009). This observation steps through the many BSM mechanical parameters in turn changing each one by incremental steps in order to try and identify the problems. At present the bulk movement parameters have been analysed (the parameters that move the BSM to the correct –order of magnitude- position and some recommendations have been made to improve the stability (specifically changing the Feed-Forward Offset and the Chop-Jiggle Coupling) of the BSM and the balance between the two chop beams. An additional test observation is planned to check for improvement and if successful fine tuning of the last 10% of the BSM motion will be improved (specifically Kp,Ki,Kd parameters). The timescale for the complete improvement and test observations may be on the order of months.

6.2 Instabilities introduced by the telescope pointing

During Point Source Mode, the telescope physically moves to nod from one position to another. If the telescope does not nod back to the correct position this could also result in an instability in the system especially for bright sources where the Jiggle pattern could be shifted off the peak of the source onto the steep Gaussian slope, thus reporting a different flux value for each nod cycle as implied by Figure 11. To investigate this, the pointing product is plotted in Figure 15 for the target Alpha Ori with the RA and Dec rotated to the spacecraft -Y,-Z plane. The observation has 12 ABBA cycles which are clearly seen. The zoomed panel on the right shows a scatter of ~ +/- 0.5", in good agreement with the figures from Herschel for a relative pointing error of 0.3". Although the pointing error is within requirements the effect of a +/- 0.5" shift on measurements of a bright source in Point Source Mode is tested in **Figure 16** where a simulated Gaussian of amplitude 5.5Jy is used to represent the target Alpha Ori (where it is known that the pointing ~5.6" away from source peak). Three points on the curve are shown: The central point at 5.6" away from the maximum and two additional points 0.5" away from either side of central point. The difference between the flux of the central point and the other two points is approximately 200mJy, i.e. a similar magnitude to, but completely independent of, the uncertainties seen with the BSM.

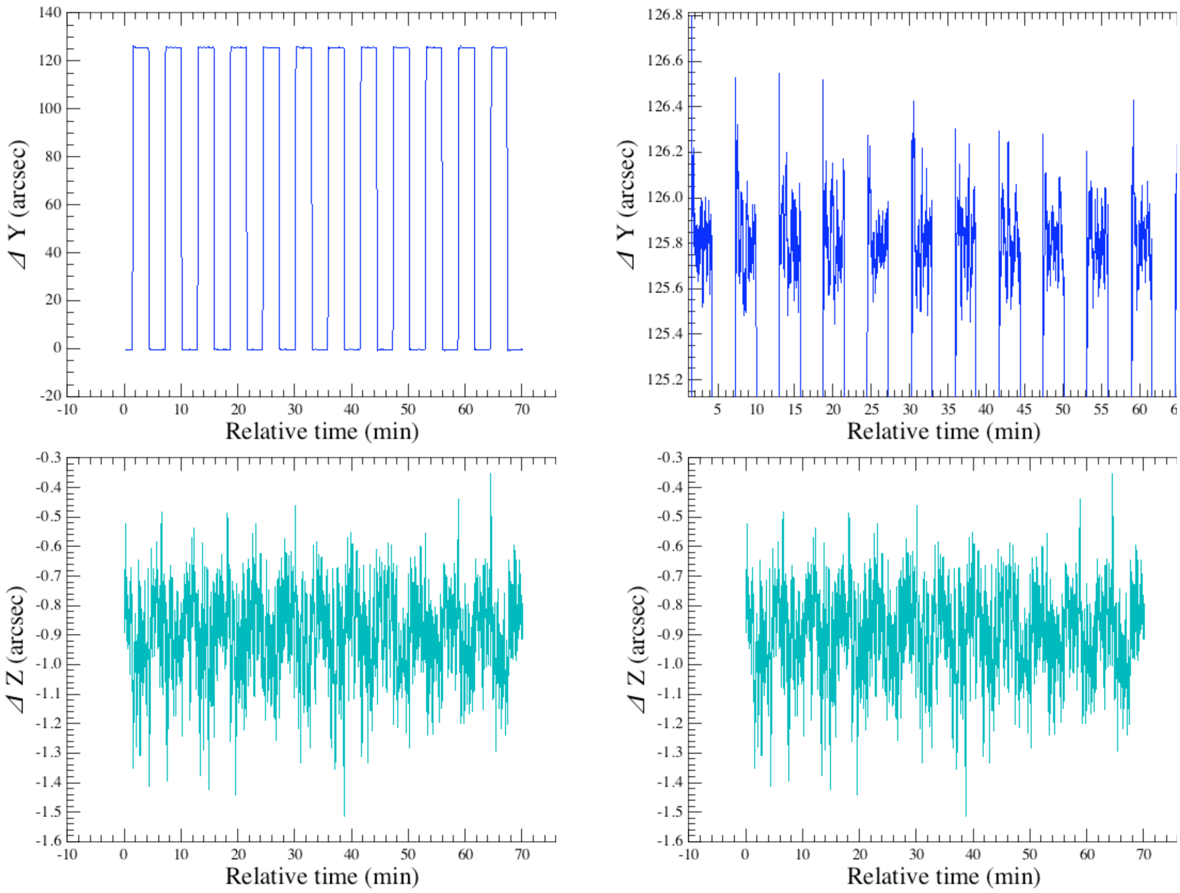

Figure 15: *The spacecraft pointing product for the target Alpha Ori with RA and Dec rotated to the spacecraft -Y,-Z plane. The observation has 12 ABBA cycles which are clearly seen. The zoomed panel on the right shows a scatter of ~ +/- 0.4", in good agreement with the figures from Herschel for a relative pointing error of 0.3"*

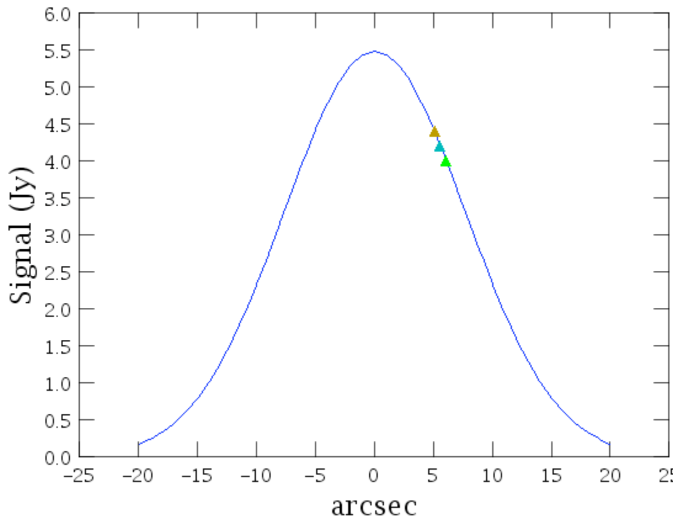

Figure 16: *Simulation of the target Alpha Ori (where it is known that the pointing ~5.6" away from source peak) with a Gaussian of amplitude 5.5Jy. Three points on the curve are shown: The central point at 5.6" away from the maximum (blue). Two additional points 0.5" away from either side of central point (brown & green). The difference between the central point flux and the other two points is 0.2 Jy.*

As an additional investigation as to the effect of any uncertainties introduced by the nominal pointing errors, in Figure 17 the two Nod A positions of an **A**BB**A** cycle are plotted. For an ideal system, the two Nod=A positions should be at the same position and measure the same signal. Figure 17 plots the signal timeline for the Level 0.5 data products (i.e. before demodulation and De-nodding) showing that there is a difference between the Nod cycle positions causing a fluctuation in measured signal of as much as 200mJy. In the right panels of Figure 17 the RA and Dec is plotted for the two Nod=A positions and whilst the Dec values are consistent with each other, the RA values show offsets of the order of an arcsec. Note that the BSM instability in both the signal and the position can also be clearly seen in the figure but that the pointing uncertainty is super-posed on top of any BSM effects.
The pointing uncertainty will introduce a fundamental limit to measurements made in the point source mode.

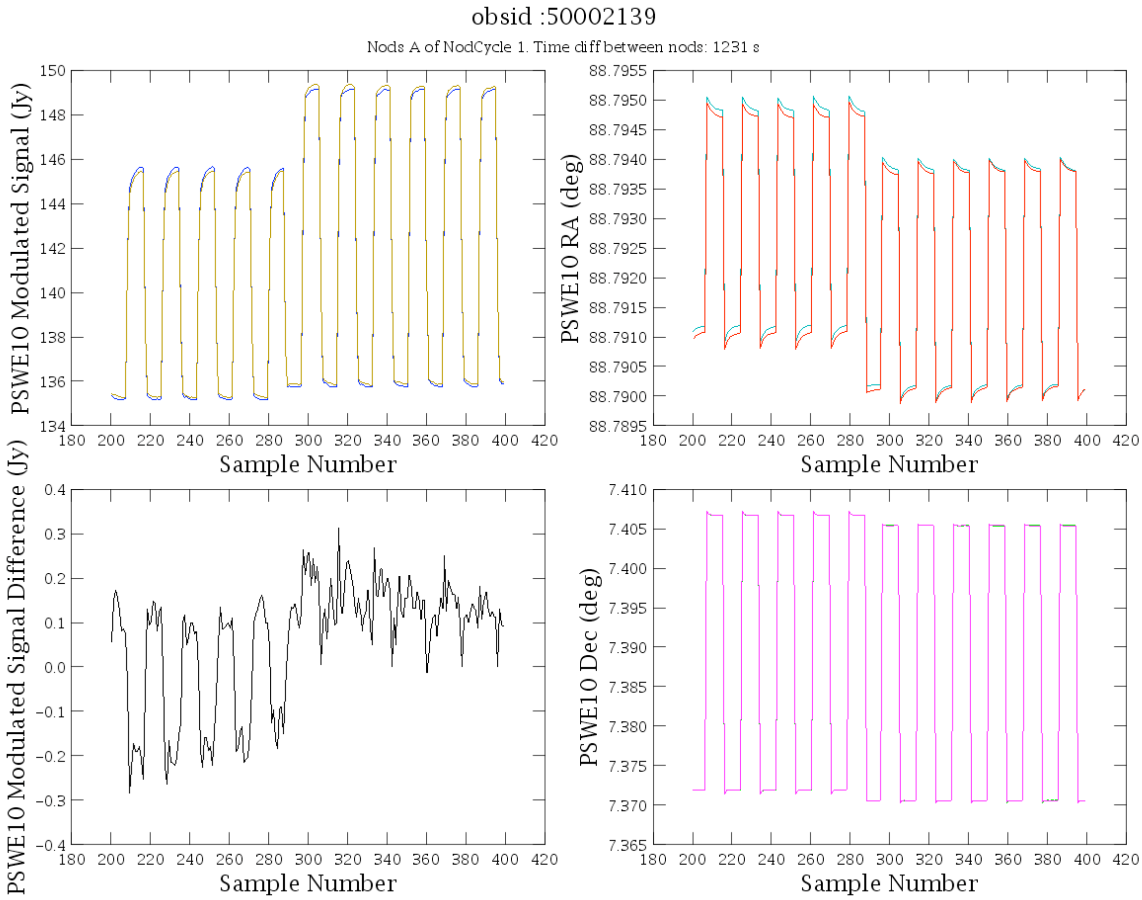

Figure 17: *A comparison of the differences in detector signal (Level 0.5 data timelines) and positional offsets for the two Nod=A positions in a nominal **A**BB**A** cycle, where ideally the two Nod=A positions should be identical. Top left panel: Level 0.5 data timelines with the two different colour lines corresponding to the two different nods, with the difference between the lines shown in the bottom right panel. Right hand panels: The RA and Dec timelines with the two different colour lines corresponding to the two different nods.*

6.3 Sensitivity Estimates

Currently, given the instability of the system it is difficult to quantify the absolute sensitivity of this observation mode. Moreover, the errors also depend on the source flux, since chopping or nodding back on to a different position on a bright (steep distribution) Gaussian source produces significant errors. As a preliminary measure of the errors in the Point Source Mode a pair of observations have been chosen which contain very large numbers of Nod-cycles (12 each). The RMS flux error is then calculated from all of the individual fluxes measured on each Nod Cycle and plotted against the source flux in **Figure 18**. The two observations plotted are for Alpha Ori (~5.1Jy) and Gamma Dra (~200mJy), and the measured RMS values are 100mJy and 8mJy respectively. Also plotted in **Figure 18** are horizontal lines corresponding to the RMS values for the 1x1 Small Scan Map Mode for a given number of scan repetitions indicating where the scan map mode becomes more efficient..

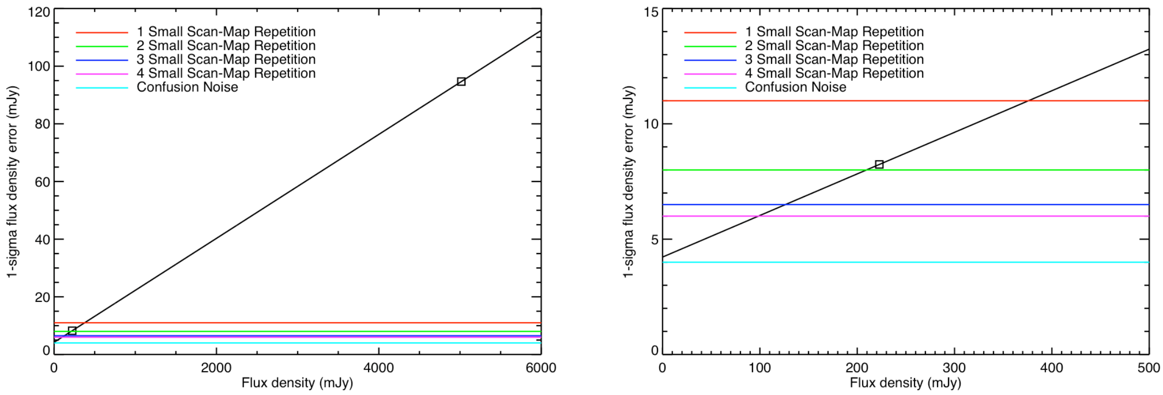

Figure 18: *Quantifying the performance of Point Source Mode by measuring the RMS flux error on multiple Nod (12) cycles of Alpha Ori (~5.1Jy) and Gamma Dra (~200mJy). A linear fit* is shown and compared with the RMS values expected for a small-scan map.

7 The future of the SPIRE Point Source Mode

7.1 Point Source Mode in Guaranteed and Open Time Proposals

Given the problems with the repeatability and the propagation of errors in the Point Source Mode a preliminary investigation has been carried out into guaranteed and open time science projects that are currently waiting to use the Point Source Mode.

The current list of projects is;

1. KPGT_kmeisenh_1: A large sample of faint quasars
2. KPGT_pharto01_1: Observations of a pair of comets
3. KPGT_smadde01_1: a sample of local galaxies
4. KPOT_bmatthew_1: Debris discs
5. KPOT_ceiroa_1: Debris discs
6. KPOT_nevans_1: a sample of stars

In the case of (1) above the targets may be near the confusion limit and the P.I. has indicated a preference to change to SPIRE Small Scan Map mode. Project (3) is also considering a Small Scan Map for the faint sources and also since background may be important. Projects (4) & (5) are also advocating a change to Small Scan Map mode since chopping on-off source can inherently introduce structure into their targets.

7.2 Summary

Currently, the Point Source Mode does not generate adequate repeatability to merit release of the AOT. Given that the total time for a Small Scan Map and a Point Source are becoming comparable (due to improvements in the mapping modes) and that the mapping modes are significantly more stable and better understood, we will reach a decision based on science goals, manpower and timescale for improvement on whether the Point Source Mode will be released or whether alternatively the mode will be replaced by Small Scan Map mode.